Pegylated Leptin Antagonist Is a Potent Orexigenic Agent: Preparation and Mechanism of Activity

Eran Elinav,* Leonora Niv-Spector,* Meirav Katz, Tulin O. Price, Mohammed Ali, Michal Yacobovitz, Gili Solomon, Shay Reicher, Jessica L. Lynch, Zamir Halpern, William A. Banks, and Arieh Gertler

Institute for Gastroenterology and Liver Disease (E.E., M.K., M.A., Z.H.), Tel Aviv Sourasky Medical Center, Tel Aviv 64239, Israel; The Robert H. Smith Faculty of Agriculture, Food, and the Environment (L.N.-S., M.Y., A.G., G.S., S.R.), The Hebrew University, Rehovot 76100, Israel; and Geriatrics Research Education and Clinical Center (T.O.P., J.L.L., W.A.B.), Veterans Affairs Medical Center-St. Louis, and Division of Geriatrics (T.O.P., J.L.L., W.A.B.), Department of Internal Medicine, Saint Louis University School of Medicine, St. Louis, Missouri 63106

Leptin, a pleiotropic adipokine, is a central regulator of appetite and weight and a key immunomodulatory protein. Although inborn leptin deficiency causes weight gain, it is unclear whether induced leptin deficiency in adult wild-type animals would be orexigenic. Previous work with a potent competitive leptin antagonist did not induce a true metabolic state of leptin deficiency in mice because of a short circulating half-life. In this study, we increased the half-life of the leptin antagonist by pegylation, which resulted in significantly increased bioavailability and retaining of antagonistic activity. Mice administered the pegylated antagonist showed a rapid and dramatic increase in food intake with weight gain. Resulting fat was confined to the mesenteric region with no accumulation in the liver. Serum cholesterol, triglyceride, and hepatic aminotransferases remained unaffected. Weight changes were reversible on cessation of leptin antagonist treatment. The mechanism of severe central leptin deficiency was found to be primarily caused by blockade of transport of circulating leptin across the blood-brain barrier with antagonisms at the arcuate nucleus playing a more minor role. Altogether we introduce a novel compound that induces central and peripheral leptin deficiency. This compound should be useful in exploring the involvement of leptin in metabolic and immune processes and could serve as a therapeutic for the treatment of cachexia. **(*Endocrinology* 150: 3083–3091, 2009)**

Leptin, a 16-kDa hormone produced mainly by fat cells, was identified by positional cloning of the *ob* gene, whose absence is responsible for the development of obesity in ob/ob mice (1). Recent evidence suggests that excess leptin levels contribute to atherosclerosis and increased risk of cardiovascular disease in obese people (2, 3). Leptin is also involved in T cell-dependent immunity and autoimmune diseases (3–5) as well as being a central mediator of liver fibrogenesis (6). Blocking leptin activity via the use of leptin antagonism may provide therapy for these disorders in addition to the potential for induction of significant weight gain in various cases of cachexia, (7–9). Rising to the challenge, we recently developed potent leptin antagonists by alanine mutagenesis of amino acids 39 to 41–42. Nevertheless, the extremely short half-life of the antagonist necessitated administration of superphysiological doses to produce clinical response and did not suffice to induce a true metabolic state of leptin deficiency (10).

Increasing the biopotency of leptin antagonist can be achieved by either increasing its affinity to the receptor or reducing its clearance from the circulation. Hormones with molecular masses similar to that of leptin are cleared primarily via the kidneys, with a half-life of only 8–30 min (11, 12). Increasing the protein's size to more than 70 kDa by attachment of a polyethylene glycol (PEG) molecule results in reduced renal clearance and consequent prolongation of its half-life. Recently several PEG-conjugated medications have proven to be superior to their unmodified parent molecules and they are now widely used in clinical practice, including peginterferon-α (chronic hepatitis C),

ISSN Print 0013-7227 ISSN Online 1945-7170
Printed in U.S.A.

doi: 10.1210/en.2008-1706 Received December 5, 2008. Accepted March 25, 2009.
First Published Online April 2, 2009
* E.E. and L.N.-S. contributed equally to this manuscript.

Abbreviations: ALD, Aldehyde; BBB, blood-brain barrier; CNS, central nervous system; %Inj/ml, percent of the injected dose in each milliliter of serum; MLA, mouse leptin antagonist; PEG, polyethylene glycol; PEG-MLA, pegylated MLA.

pegfilgrastim (neutropenia), and pegvisomant (acromegaly) (13, 14). Improved efficacy is attributed to better stability, greater protection against proteolytic degradation, longer *in vivo* circulating half-lives, and lower clearance. Whereas reduction in *in vitro* activity is routinely noted after pegylation, the significantly improved half-life compensates for this effect, resulting in a net enhancement of biological activity (15).

In this manuscript, we describe the development of a pegylated leptin antagonist and demonstrate that it induces a reversible state of leptin deficiency in adult animals. Furthermore, we study the mechanisms governing this antagonistic effect.

Materials and Methods

Pegylation of human leptin and human and mouse leptin antagonists

Activated PEG polymers [branched mPEG2-NHS (*N*-hydroxysuccinimide) 40 kDa and mPEG-SMB (substituted α-methylbutanoate) of 20 and 30 kDa, branched mPEG2-butyryl-aldehyde (ALD) 40 kDa, and linear mPEG-butyryl-ALD 20 kDa] were purchased from Nektar Therapeutics (San Carlos, CA), and mPEG-propionyl-ALD 20 kDa was purchased from Jenkem Technology USA Inc. (Allen, TX). Random pegylation of primary amines was carried out by dissolving leptin or leptin antagonist (3 mg/ml; 5–10 ml) in 0.1 M Na-borate buffer (pH 5) that was conjugated with activated PEG polymers with PEG masses of 20, 30, and 40 kDa, according to the manufacturers' instructions. Protein concentrations were determined by absorbance at 280 nm using an extinction coefficient (for 0.1%) of 0.885 for human and 0.200 mg/ml for mouse leptin or leptin antagonists. Those values apply to the protein part of the pegylated product.

N-terminal amino acid analysis

Human or mouse leptins or their respective antagonists were subjected to SDS-PAGE and electroblotted onto a polyvinyl difluoride membrane (Bio-Rad, Hercules, CA) for direct N-terminal sequencing by Edman degradation. Protein microsequencing was performed on an ABI Precise model 491 sequencer system (Applied Biosystems, Foster City, CA).

Molecular mass determination

Leptin and pegylated leptin conjugates were analyzed by matrix-assisted laser desorption ionization-time of flight (Reflex III; Bruker, Ettingen, Germany) and 12% SDS-PAGE, and apparent molecular mass (Stoke's radius) of the compounds was estimated by Superdex 200 HR (GE Healthcare, Buckinghamshire, UK) 10/300 gel-filtration column chromatography. All proteins consisted of greater than 95% monomers and had very low quantities of dimers.

Binding and proliferation assays

Radiolabeled human ^{125}I-leptin prepared as described previously (16) served as a ligand, and all other unlabeled pegylated leptins or leptin antagonists as competitors. The experiments were conducted with homogenates of BAF/3 cells stably transfected with the long form of the human leptin receptor as described previously (17). The proliferation rate of the same cells was used to estimate self- and antagonistic activity of pegylated and nonpegylated leptin or leptin antagonists as previously described (16).

In vivo experiments

In all feeding experiments, female C57BLmice were administered with mouse leptin antagonist (MLA) or pegylated MLA (PEG-MLA) (12.5–50 mg/kg · d) or leptin (1 mg/kg · d) sc. In the weaning experiments, the treatment was ceased after 11 d and reversibility of the leptin deficiency phenotype was recorded. In an additional experiment aimed to statistically evaluate simultaneous weight gain and food intake through a 4-wk period, 12 mice per treatment were housed in three cages. Food intake and weight gain were recorded twice a week for 4 wk and averaged for a period of 3–4 d. In all experiments animals were maintained under 12-h light, 12-h dark cycles, in accordance with regulations of the institutional animal and care authority of the Tel Aviv Sourasky Medical Center.

Total body and hepatic lipid analysis

Carcass total and hepatic fat analysis was performed using chloroform/MeOH dissolution, as previously described (18).

Measurement of influx into the brain

In male CD-1 mice, multiple time-regression analysis was applied as previously detailed (19, 20) to calculate the unidirectional blood-to-brain influx rate of MLA or PEG-MLA. To measure inhibition of leptin transport, 3×10^5 cpm of ^{131}I-leptin was injected iv with 30 μg/mouse of unlabeled PEG-MLA or sc with 25 mg/kg PEG-MLA or saline 4 h before measurement of blood-to-brain transport. The whole brain was removed at 1–10 min after injection of the ^{131}I-leptin and processed. Results were expressed as brain to serum ratios. To determine whether MLA is able to inhibit entry of ^{131}I-leptin into the brain, 1 μg/mouse of nonradioactive MLA was included in the iv injection of some mice.

Clearance from serum

To determine the rate of clearance of ^{131}I-PEG-MLA or ^{131}I-MLA from the serum, results were expressed as percent of the injected dose in each milliliter of serum (%Inj/ml) and these values were plotted against time (minutes). The %Inj/ml was determined by the equation: %Inj/ml = 100(counts per minute per milliliter serum)/(counts per minute per injection).

Stability of ^{131}I-PEG-MLA in blood and brain by acid precipitation

Mice were injected into the left jugular vein with 0.2 ml lactated Ringer's solution-BSA containing 3×10^5 cpm of ^{131}I-PEG-MLA. Arterial blood and brain were collected at 5, 20, 60, 480, 1080, and 1440 min after iv injection, acid precipitated, and measured as previously described (21). The percentage of radioactivity precipitated by acid in the serum and brain was calculated by the following formula: 100[(pellet counts per minute)/(pellet counts per minute + supernatant counts per minute)]. *Ex vivo* degradation was corrected for by dividing the values for the biological samples by the values for the processing controls.

Uptake into brain regions

A total 0.2 ml LR-BSA containing 8×10^5 cpm of ^{131}I-PEG-MLA and ^{125}I-albumin were injected into the left jugular vein. After blood was collected from the right abdominal aorta, mice received an intracardial perfusion of 20 ml lactated Ringer's solution to clear the cerebral vasculature immediately and 5, 30, 60, 120, 240, 360, and 480 min after iv injection. Mice were decapitated, and the brain was removed and dissected on ice into three regions (hypothalamus, frontal cortex, and cerebellum). Each region was weighed and the radioactivity was determined. Values for whole brain were calculated by adding the regional levels of radioactivity and regional weights. The brain to serum ratios (microliters per gram) for all regions and the whole brain were calculated. To correct for the vascular space, the radioactivity of ^{125}I-albumin in the brain regions was measured simultaneously with ^{131}I-PEG-MLA, and the value of ΔPEG-MLA = (^{131}I-PEG-MLA) − (^{125}I-albumin) reported.

Capillary depletion

The capillary depletion method (22, 23) modified for mice was performed to determine whether the ^{131}I-PEG-MLA completely crosses the

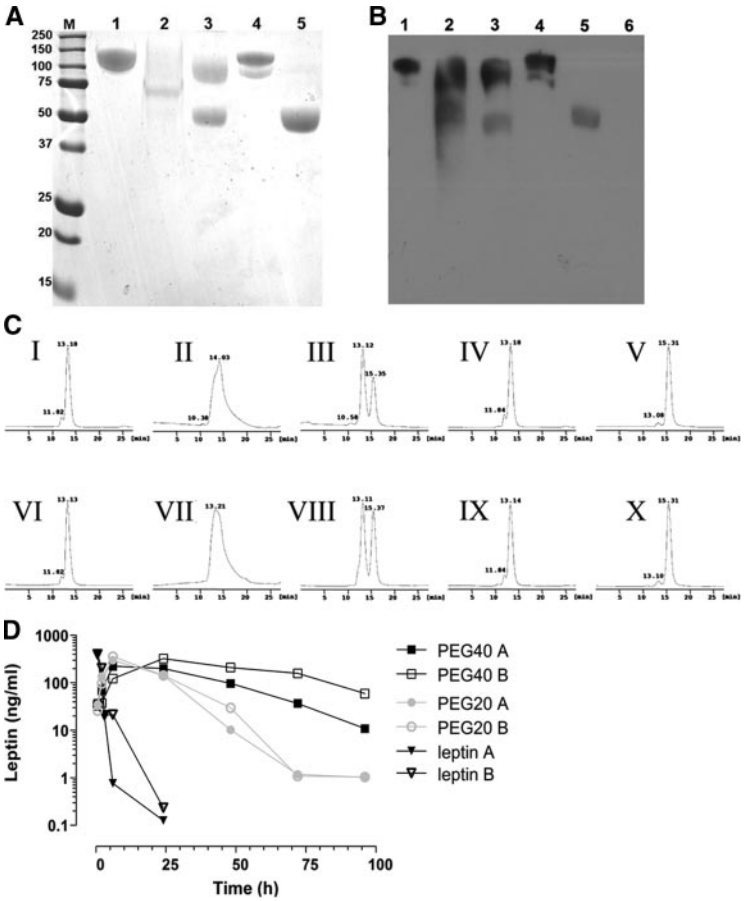

FIG. 1. Chemical characterization of pegylated leptins and leptin antagonists. A, SDS-PAGE analysis of pegylated proteins stained with Coomassie Blue. B, Western blotting of pegylated leptins with AGP3 monoclonal antibody directed against PEG. Lanes: M, Molecular weight marker proteins; 1, branched mPEG2-NHS 40 kDa; 2, mPEG-SMB 30 kDa; 3, mPEG-SMB 20 kDa; 4, branched mPEG2-butyr-ALD 40 kDa; 5, mPEG-butyr-ALD 20 kDa; 6, non-pegylated human leptin (only in B). C, Purity determination of the pegylated leptins by gel-filtration analysis. Pegylated WT leptins (I–V) and pegylated leptin antagonists (VI–X). I and VI, branched mPEG2-NHS 40 kDa; II and VII, mPEG-SMB 30 kDa; III and VIII,- mPEG-SMB 20 kDa; IV and IX, branched mPEG2-butyr-ALD 40 kDa; V and X, mPEG-butyr-ALD 20 kDa. The column was calibrated with leptin (16 kDa), chicken leptin binding domain (chLBD, 24.5 kDa) leptin-chLBD complex (40.5 kDa), BSA (66 kDa), bovine IgG monomer (150 kDa), and dimer (300 kDa). D, Serum levels of recombinant human nonpegylated leptin (*open* and *filled triangles*), human leptin pegylated with mPEG2-NHS 40 kDa (*open* and *filled squares*) or with mPEG-butyr-ALD 20 kDa (*open* and *filled circles*) after a single sc injection of 20 μg protein/mouse. Serum levels of the proteins were measured by ELISA. Data are means of duplicate wells for two mice (A and B), and the experiment was repeated twice.

capillary wall of the blood-brain barrier (BBB) to enter the brain parenchyma.

Detection of PEG-MLA in brain tissue by RIA

The RIA kit for murine leptin (Linco, St. Charles, MO) was used to detect PEG-MLA in a serial dilution of PEG-MLA from 0.313 to 20 ng/ml. To determine whether PEG-MLA had entered the brain, mice (n = 10) were injected sc with saline or 25 μg/g PEG-MLA. After 60 min, brains were removed, homogenized in 1% BSA in lactated Ringer's solution, and centrifuged at 5400 $\times$ *g* for 15 min. A measured amount of supernatant was lyophilized and then reconstituted in 250 μl RIA buffer and assayed with the RIA kit. The results for the PEG-MLA mice were multiplied by a factor of two as the dose-response curve indicated that the immunoactivity of PEG-MLA was 50% that of mouse leptin.

Measurement of brain-to-blood efflux rate

A method previously described to quantify the rate of transport from brain to blood was used (24). To test for self-inhibition of transport in other mice, nonradioactive PEG-MLA (1 μg/mouse) was included in the injection, and the brain was removed 10 min later. Results were expressed as the mean percentage of the radioactivity injected intracerebroventricular that was retained per gram of whole brain.

In vivo imaging studies

To follow the distribution of PEG-MLA or MLA, both were tagged with Alexa Fluor 680 (Invitrogen, Carlsbad, CA) and followed with a whole-body-cooled charge-coupled device camera (IVIS 100 series imaging system; Xenogen, Alameda, CA), as previously described (25).

Statistical analysis

Statistical evaluation in multigroup experiments was performed using the ANOVA parametric tests, followed by *post hoc* analysis. In two group experiments (such as the fluorescent *in vivo* imaging studies) unpaired Student's *t* test was used. $P < 0.05$ was considered significant.

Results

Preparation of pegylated leptin and leptin antagonists

For the pegylation of human leptin and leptin antagonists, we used five PEG reagents, three reacting with primary amines (mPEG2-NHS, 40 kDa; mPEG-SMB 20 and 30 kDa) and two reacting with the N-terminal α-amino group of the protein in the presence of a reducing reagent sodium cyanoborohydride (branched mPEG2-butyr-ALD, 40 kDa, and linear mPEG-butyr-ALD, 20 kDa, or mPEG-propionyl-ALD, 20 kDa). Site of pegylation was validated by sequencing the five N-terminal amino acids, which were detected only in the non-N-terminal pegylated compounds and not in N-terminal pegylated proteins (data not shown). The SDS-PAGE profiles of the purified pegylated proteins were determined by Coomassie Blue staining (Fig. 1A) and confirmed using Western blotting with anti-PEG antibody (Fig. 1B). PEG-leptin's electrophoretic mobility was considerably reduced because of PEG's large hydrodynamic volume resulting in a higher molecular mass compared with the calculated molecular weight (supplemental Table 1, published as supplemental data on The Endocrine Society's Journals Online web site at http://endo.endojournals.org). Similar results were obtained with leptin antagonist pegylated by the five reagents under identical conditions (data not shown).

The purity and homogeneity of the pegylated leptins (Fig. 1C, panels I–V) and pegylated leptin antagonists (Fig. 1C, panels VI–X) were documented by gel-filtration chromatography, yielding main peak consisting of greater than 95% monomer. After pegylation of leptin or its antagonist with mPEG-SMB, 20 kDa, two fractions were observed (Fig. 1C, panels III and VIII, respectively), confirming the former results. To validate these findings, all 10 preparations were subjected to matrix-assisted laser desorption ionization-time of flight mass spectrometry (supplemental Table 2). Similar results obtained with each of the five pegylated antagonists (not shown) and were found to

be close to the predicted theoretical molecular mass values, whereas the corresponding values obtained by SDS-PAGE and gel filtration were, respectively, 1.4- to 2.1- and 6.0- to 7.1-fold higher.

Determination of the *in vitro* antagonistic activity of pegylated leptin antagonists

To study whether the pegylated leptin and leptin antagonists retain their binding activities, binding-competition assays were performed with homogenates of BAF/3 cells stably transfected with the long form of human leptin receptor (16). Radiolabeled ^{125}I-human leptin served as the ligand, and nonradiolabeled pegylated and nonpegylated leptins and leptin antagonists served as competitors. The resulting binding activity of pegylated leptin or leptin antagonists varied from 3.8 to 16.8% compared with the nonpegylated protein (supplemental Table 2). The highest binding activity was found with leptin or its antagonist conjugated with 20 kDa mPEG-butyr-ALD. Similarly, antagonistic activity of pegylated leptin or its antagonist, as determined by the proliferation rate of leptin-sensitive BAF/3 cells, varied from about 3 to 19.5% of the respective nonpegylated proteins, the greatest biological activity recorded with leptin and leptin antagonist conjugated with mPEG-butyr-ALD, 20 kDa (supplemental Table 2). The activities decreased with PEG molecular mass and were well correlated with the binding results. Similar binding and proliferation results were obtained with PEG-MLA (data not shown).

Determination of *in vivo* half-life of pegylated leptin

For *in vivo* determination of the half-life of pegylated leptin and leptin antagonists, mice received sc injections of either human leptin or its pegylated conjugates mPEG2-NHS, 40 kDa, and mPEG-butyr-ALD, 20 kDa. Leptin levels were determined using a human leptin ELISA kit that was not cross-reactive with the endogenous mouse leptin (Fig. 1D). Leptin was cleared rapidly, disappearing after 24 h. In contrast, both pegylated bioconjugates exhibited markedly enhanced persistence, with 35- and 13.4-fold increases in half-life in comparison with nonpegylated leptin, respectively. PEG-ALD, 20 kDa, MLA featured the best overall combination of elongated half-life and the least reduced biological activity and was thus used in all subsequent *in vivo* experiments. Preparation of homologous reagent for *in vivo* experiments in mice PEG-MLA was upscaled to batches of 120–160 mg of protein.

Administration of PEG-MLA results in a state of severe leptin deficiency

Daily injections of PEG-MLA resulted in significant weight gain starting after the first day of injection (Fig. 2A), which were similarly significant with three different doses of PEG-MLA relative to controls ($P < 0.05$ on d 2 to $P < 0.001$ on d 7). Administration of MLA resulted in a mild weight gain that was apparent only after 4 d and reached statistical significance ($P < 0.05$) at the highest 25 and 50 mg/kg · d doses after 5 d. A typical difference in body sizes is presented in Fig. 2B. In contrast, administration of leptin (given at 1 mg/kg · d) resulted in a nonstatistically significant weight reduction. Weight gain in PEG-MLA-administered mice was associated with a significant increase in food consumption (Fig. 2C), from 2.40 ± 0.10 g/mouse · d (mean ± SEM) in the three groups of MLA-administered mice to 3.24 ± 0.09 g/mouse · d in the three groups of PEG-MLA-administered mice ($P < 0.001$). MLA treatment was associated with a nonstatistically significant trend of elevated food intake. As is shown in supplemental Fig. 1, PEG-MLA-induced enhancement in food intake was already evident on d 1–3 and gradually increased until d 11. Thereafter the food intake was lowered and became statistically nondifferent from control, whereas weight gain was maintained. In another experiment cessation of PEG-MLA administration after 12 d of treatment resulted in a complete reversal of weight gain (Fig. 2D).

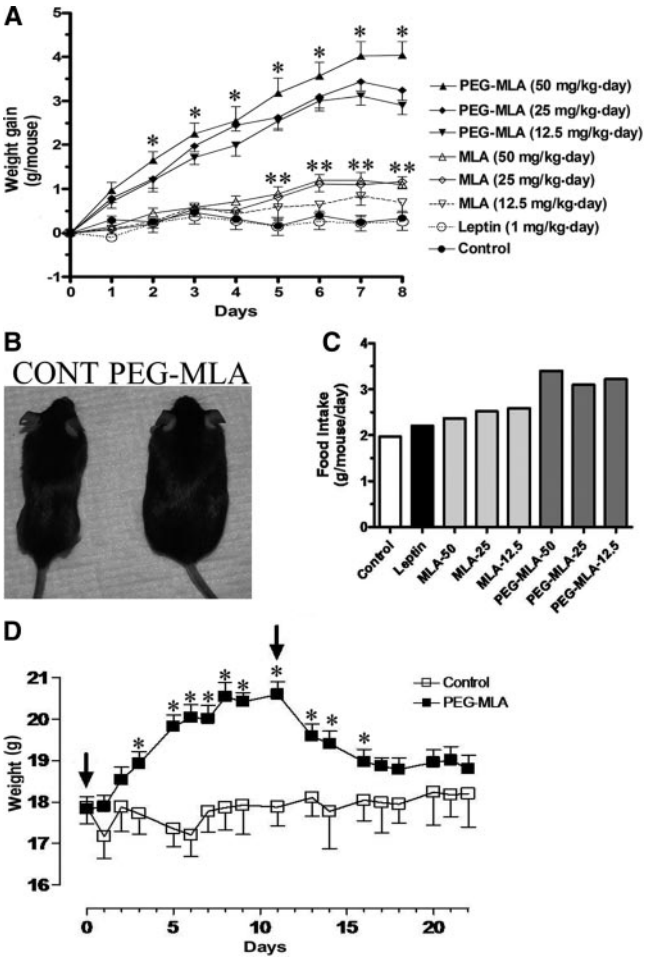

FIG. 2 Induction of leptin deficiency by pegylated leptin antagonist. A, WT C57Bl mice (n = 4) were administered sc at the specified doses of PEG-MLA or leptin, and weight was recorded daily for a total of 8 d. Mice administered with all three doses of PEG-MLA featured a significantly increased weight gain as compared with either MLA or controls (*, $P < 0.05$). Only mice administered 25 and 50 mg/kg · d MLA doses for more than 5 d developed significantly increased weight gain as compared to controls (**, $P < 0.05$). B, Appearance of representative control (CONT) and PEG-MLA-administered mice. C, Average daily food intake of mice administered specified doses of PEG-MLA or leptin during the 8-d period. D, For determination of the reversibility of leptin deficiency, WT C57Bl mice (n = 6) were administered sc with 25 mg/kg · d PEG-MLA or vehicle for 11 d, followed by cessation of treatment (start and finish days of treatment are marked by *arrows*). PEG-MLA-treated mice featured a significantly increased weight gain as compared with controls (*, $P < 0.05$). Cessation of treatment was associated with return to baseline weight levels within a 1-wk period.

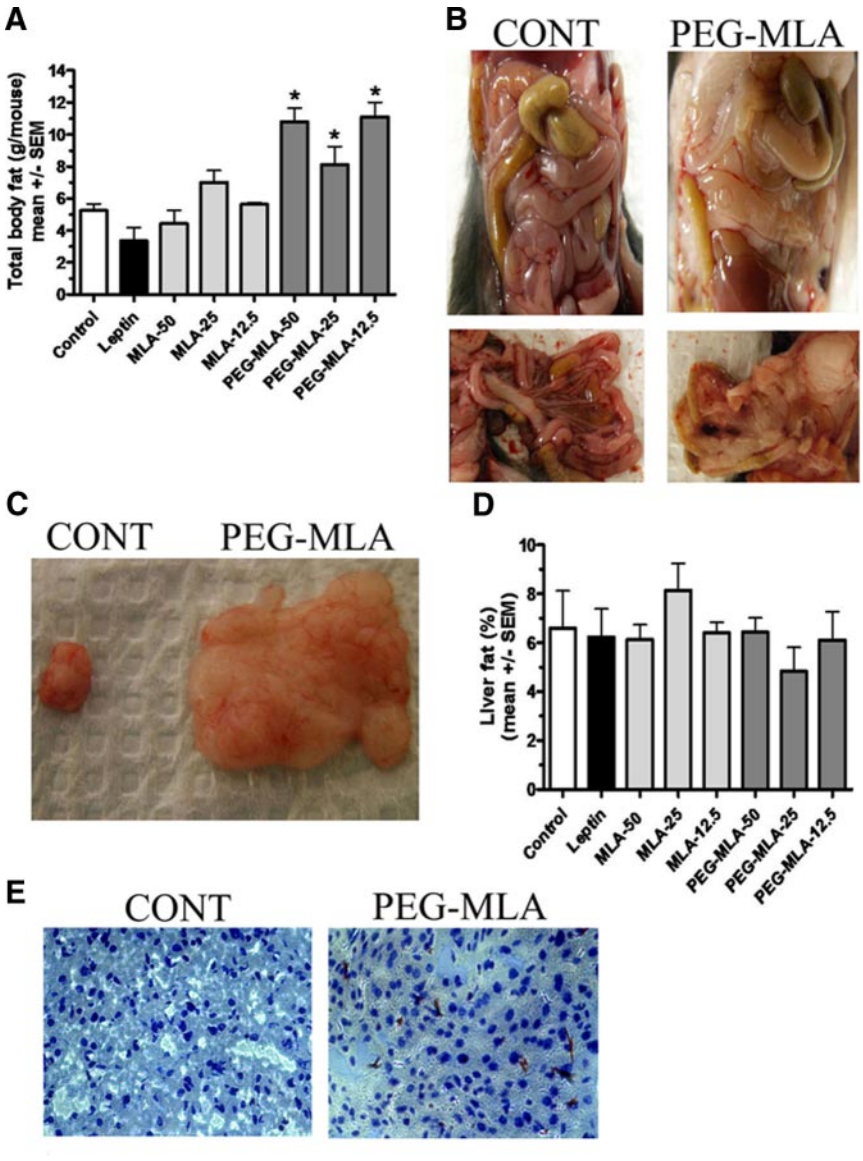

FIG. 3 Pegylated leptin antagonist-induced fat accumulation. A, WT C57Bl mice (n = 7) were administered sc at the specified doses of PEG-MLA or leptin, killed after 8 d, and total body fat content and hepatic fat content were measured using choloroform:methanol dissolution. PEG-MLA-administered mice featured a significantly increased total body fat content (*, $P < 0.05$). B, Mesenteric fat distribution from representative control and PEG-MLA-administered mice. C, Total amount of mesenteric fat dissected from representative control and PEG-MLA-administered mice. D, Hepatic fat content in mice was measured as described above. No significant differences were noted between PEG-MLA and leptin-administered or control mice (P = NS). E, Representative Oil-red-O sections from livers of representative control and PEG-MLA-administered mice. No significant fat deposition was noted in any of the mouse groups.

Weight gain was largely caused by a significant increase in body fat, with a massive 4- to 6-g accumulation of fat compared with controls ($P < 0.05$, Fig. 3A). No such fat accumulation was observed in MLA-injected mice (P = NS). The fat distribution was mostly confined to the mesenteric compartment (Fig. 3, B and C), with sparing of the liver (Fig. 3, D and E) and sc tissue (data not shown). Because more than 90% of fat accumulation was found within the mesenteric region, we estimated the amount of mesenteric fat to directly correlate with the weight gain noted in Fig. 3A. Treatments with PEG-MLA, MLA or leptin were not associated with any pathological findings or changes in total cholesterol, triglyceride or hepatic aminotransferase activity compared with controls (P = NS, data not shown).

Fluorescently labeled pegylated leptin antagonist displays prolonged peripheral distribution, with no observed penetration into the central nervous system (CNS)

To follow PEG-MLA distribution in the body, it was conjugated to Alexa Fluor 680 (Invitrogen) and was continuously tracked using the IVIS *in vivo* imaging system (Xenogen). As demonstrated in Fig. 4A (*upper panel*), MLA rapidly distributed throughout the body but then was quickly cleared, its signal disappearing 1 h after administration. In contrast, PEG-MLA was mainly observed in the mediastinal region and kidneys (Fig. 4A, *lower panel*) as well as the urinary bladder and to a lesser extent the liver (data not shown) for more than 7 h after its administration. Even 24 h after administration, PEG-MLA could be imaged in the explanted lungs, kidneys, and urinary bladder (Fig. 4B). Signal quantification revealed significant enhancement of PEG-MLA fluorescence intensity from 4 h after injection, and its persistence at 24 h in explanted organs (average radiance of 6.02 ± 0.89, 6.67 ± 0.73, 5.00 ± 1.38 *vs.* 0.42 ± 1.25, 0.00 ± 0.56, 0.00 ± 1.32 for the 4, 7, and 24 h PEG-MLA and MLA-administered groups, respectively, $P < 0.001$ at all indicated time points). Whereas fluorescence could be seen in the area including the CNS after MLA administration (at the 5 and 30 min time points, Fig. 4C, *upper panel*), no fluorescence could be seen within this area in mice receiving PEG-MLA (Fig. 4C, *lower panel*), indicating none or only slight penetration, below the level of fluorescence detection.

Induction of leptin deficiency by PEG-MLA is mediated by inhibition of both leptin transport through the BBB and its CNS activity

To study the mechanism governing the *in vivo* inhibitory activity of MLA and PEG-MLA, both were labeled with ^{131}I and administered iv to mice. As shown in Fig. 5A, there was no correlation between the brain to serum ratios of ^{131}I-PEG-MLA and exposure time during the study period (2–75 min after iv injection in mice), indicating lack of measurable blood-to-brain transport during this period. In contrast, a linear relationship was found between brain to serum ratios and exposure time for ^{131}I-MLA between 2 and 65 min after iv injection, indicating that ^{131}I-MLA crossed the BBB in the blood-to-brain direction (Fig. 5B). The unidirectional blood-to-brain influx rate for ^{131}I-MLA was 0.277 ± 0.028 μl/g · min, and the initial volume of distri-

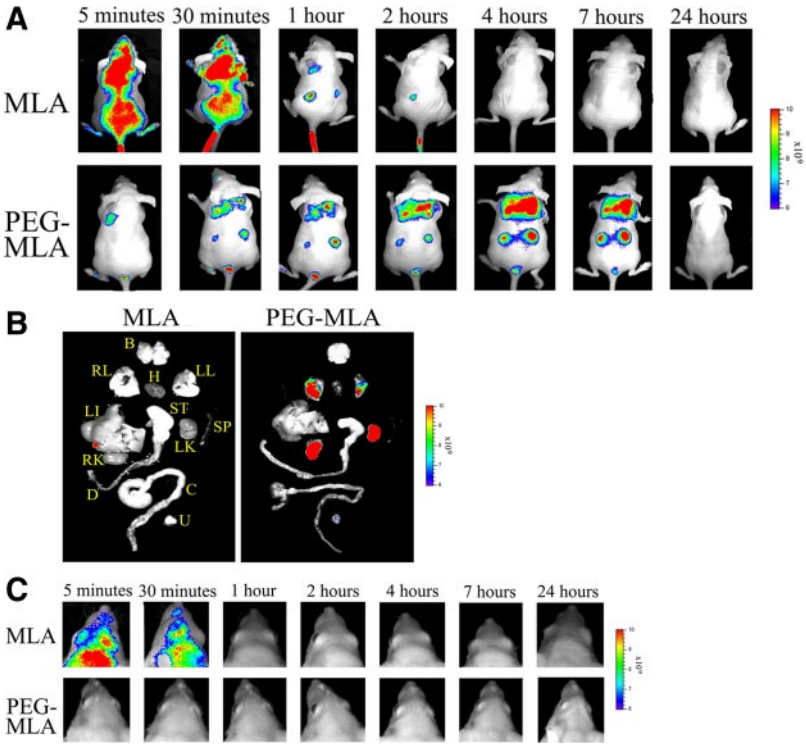

FIG. 4. *In vivo* distribution of pegylated leptin antagonist. A, *In vivo* imaging of WT mice receiving 600 μg iv Alexa Fluor 680-labeled MLA or PEG-MLA (n = 2). Mice were subjected to whole-body imaging (IVIS 100 Series Imaging System) at the indicated intervals. A single representative mouse is shown at all time points. Two independent experiments were performed, with similar results. B, *In vivo* imaging of explanted organs from mice in A, 24 h after injection. B, Brain; RL and LL, right and left lungs, respectively; H, heart; Li, liver; ST, stomach; SP, spleen; RK and LK, right and left kidney, respectively; D, duodenum; C, colon; U, urinary bladder. C, *In vivo* imaging indicating brain uptake of either MLA or PEG-MLA at the indicated time points.

bution was 14.01 ± 1.02 μl/g ($P < 0.0001$, r = 0.93, n = 2 mice per time point).

The early phase of ^{131}I-PEG-MLA and ^{131}I-MLA clearance from the serum after injection into the jugular vein followed first-order kinetics (Fig. 5, C and D, respectively). Linear regression analysis of that early phase (Fig. 5, C and D, *insets*) showed a statistically significant relation between log of radioactivity level in arterial serum and time (r = 0.74, $P < 0.0001$, n = 2–3 mice per time point). The half-time disappearance of ^{131}I-PEG-MLA in blood as calculated from the inverse of the slope of this relation was 66.7 min, compared with 18.0 min for ^{131}I-MLA (r = 0.88, $P < 0.0001$, n = 2 mice per time point).

To test whether PEG-MLA exerts its effects via inhibition of blood-to-brain leptin transport, we included 30 μg of unlabeled PEG-MLA per mouse in the ivinjection of ^{131}I-leptin. Unlabeled PEG-MLA significantly attenuated blood-to-brain transport of ^{131}I-leptin ($P = 0.018$, n = 14, Fig. 6A). Similar alteration of leptin blood-to-brain transport was noted with sc administration of PEG-MLA, which significantly reduced ^{131}I-leptin transport ($P = 0.02$, n = 8) relative to saline controls (Fig. 6B). As with PEG-MLA, the addition of 1 μg/mouse nonpegylated MLA reduced the brain to serum ratio of ^{131}I-leptin and hence inhibited the transport of ^{131}I-leptin. The brain to serum ratio for ^{131}I-leptin (labeled only) was 24.3 ± 3.8 μl/g, whereas that of I-leptin + unlabeled (nonradioactive) MLA was 15.2 ± 2.9 μl/g 10 min after iv injection (n = 10 mice/group, $P < 0.0001$). To determine the *in vivo* stability of ^{131}I-PEG-MLA in serum and brain at 5, 20, 60, 480, 1080, and 1440 min after iv injection, acid precipitation was performed. Supplemental Table 3 shows that most of the degradation of ^{131}I-PEG-MLA occurred more than 8 and 18 h after iv administration into the brain and serum, respectively.

When followed over time, ^{131}I-PEG-MLA slowly entered different regions of the CNS, including the hypothalamus, frontal cortex, and cerebellum (Fig. 6, C–F), all at a considerably lower rate than leptin. The highest uptake rate of ^{131}I-PEG-MLA was demonstrated in the hypothalamus (0.0144 ± 0.007 μl/g · min), in which it was 40 times lower than the influx rate of native leptin, even after correction for vascular space by subtraction of ^{125}I-albumin. To study the actual passage of ^{131}I-PEG-MLA across the brain endothelial barrier into the brain parenchymal space, capillary depletion was conducted 8 h after iv coinjection of ^{131}I-PEG-MLA and ^{125}I-albumin, the latter serving to correct for any contamination by residual serum: 80% of the ^{131}I-PEG-MLA entered the brain parenchyma during the 8-h study period (2.20 ± 0.57 μl/g), with only 20% remaining in the capillary fraction (0.52 ± 0.17 μl/g, $P = 0.0375$, n = 5). To confirm these results and estimate the brain concentrations of PEG-MLA relative to those of endogenous leptin, mice (n = 10) were sc administered 25 μg/g of PEG-MLA or vehicle only, followed 1 h later with measurement by RIA of brain PEG-MLA or leptin, respectively. Mean brain level of leptin antagonist in PEG-MLA-treated mice was 12.4 ± 0.42 ng/g brain, compared with 0.17 ± 0.06 ng endogenous leptin per gram brain in vehicle-treated mice ($P < 0.001$, Fig. 6G). BBB permeability was not changed in mice injected with pegylated leptin.

Brain-to-blood efflux of ^{131}I-PEG-MLA was measured after intracerebroventricular injection and demonstrated a statistically significant relationship between log brain counts per minute and time, proving a significant efflux of ^{131}I-PEG-MLA from the brain (r = 0.93, n = 12, $P < 0.0001$, Fig. 6H). The half-time disappearance rate, calculated from the slope of this relation was 20.94 min. The addition of nonradioactive PEG-MLA did not inhibit ^{131}I-PEG-MLA efflux (25.8 ± 8.0 and 24.0 ± 7.5% for ^{131}I-PEG-MLA and ^{131}I-PEG-MLA + nonradioactive PEG-MLA, respectively, Fig. 6I).

Discussion

We developed a long-acting leptin antagonist (PEG-MLA) that enables, for the first time, reversible induction of a state of leptin deficiency in an adult, nontransgenic setting. We demonstrate that: 1) pegylation of leptin antagonist significantly lengthens its half-life and overall *in vivo* biological activity; 2) administration of PEG-MLA to mice results in significant weight gain, mediated

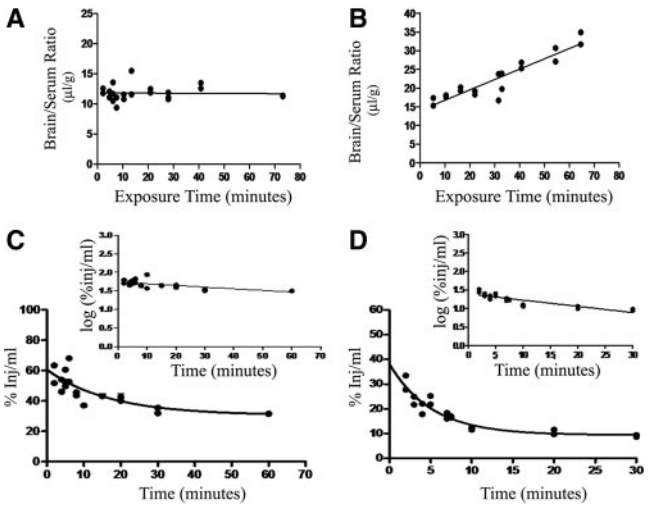

FIG. 5. Comparison of blood-to-brain transport and clearance of MLA and PEG-MLA. A, Multiple time-regression analysis of ^{131}I-PEG-MLA after iv injection. The lack of a statistically significant correlation between brain-to-serum ratios and Expt (*i.e.* a flat line) indicates a lack of measurable transfer across the BBB during this time period. B, Multiple time-regression analysis of ^{131}I-MLA after iv injection. A significant correlation between brain-to-serum ratios and Expt indicates measurable transfer across the BBB. The unidirectional blood-to-brain influx rate was measured to be 0.277 μl/g · min. C, Clearance from blood after iv injection of ^{131}I-PEG-MLA. *Inset*, Data plotted in log-linear format. Calculated half-time disappearance from blood was 66.7 min ($P < 0.0001$, r = 0.73, n = 2–3 mice per time point). D, Clearance from blood after iv injection of ^{131}I-MLA. *Inset*, Data plotted in log-linear format. Calculated half-time disappearance from blood was 18.0 min ($P < 0.0001$, r = 0.88, n = 2 mice per time point).

by food consumption; 3) PEG-MLA induces the accumulation of adipose tissue mainly in the mesenteric region and spares the liver; 4) PEG-MLA-induced leptin inhibition is mainly mediated by competitive inhibition of endogenous leptin transport through the BBB.

Taken together, the results described in this study show the possibility of reversibly inducing clinically significant leptin deficiency for both research and therapeutic purposes and suggest a mechanism for the *in vivo* activity of pegylated leptin antagonist. The pegylated compounds featured reduced *in vitro* binding properties and biological activities that were well compensated by an elongated half-life, overcoming the deficits in receptor-binding affinity and resulting in significantly enhanced overall *in vivo* activity (26, 27).

After PEG-MLA-induced weight gain and increase in food consumption, weight was stabilized and the appetite reduced to the level slightly higher but not significantly different from the control (Fig. 2D and supplemental Fig. 1), a phenomenon that may result from compensatory development of a state of enhanced leptin sensitivity, in contrast to the relative leptin resistance that is noted in hyperleptinemic morbid obesity (28). The PEG-MLA-associated adipose tissue distribution was confined to the mesenteric region. This indicates the possible existence of regional leptin-associated mechanisms for control of fat production. Indeed, leptin levels were shown to correlate with abdominal obesity in obese adults and children as well as nonobese women (29–32). It has been suggested that regional levels of leptin, which is catecholamine sensitive, may be affected by differences in catecholamine concentrations in different adipose regions, thus contributing to its localized effects (33). The phenotypic differences in hepatic fat accumulation between leptin-deficient ob/ob mice and PEG-MLA-administered wild-type mice may stem from the excessive duration of the leptin deficiency and its associated developmental aberrations in the genetic model, as opposed to residual leptin activity in PEG-MLA-treated animals. Interestingly, PEG-MLA was found to accumulate in the lungs (Fig. 4). This unexplained phenomenon is under current study and may result from accumulation of PEG-MLA within alveolar macrophages.

PEG-MLA was found to block circulating leptin from crossing the BBB, an action that would attenuate the anorectic action of endogenous leptin. Nonpegylated MLA was also found to effectively block leptin transport into the brain. However, at present the difference in the MLA and PEG-MLA transport through the BBB is not fully understood. In fact, pegylated leptin that was conjugated to Alexa Fluor 680 (Invitrogen) was found to rapidly penetrate the BBB (Elinav E., L. Niv-Spector, and A. Gertler, unpublished data). Therefore, a combination of PEG domain and conversion of the agonist into antagonist may account for the inhibited BBB penetration. Further investigation is needed to fully elucidate the mechanism of this phenomenon. ^{131}I-PEG-MLA featured a slow rate of efflux from the CNS and lack of inhibition by nonlabeled PEG-MLA, suggesting that PEG-MLA exits the brain primarily with the reabsorption of cerebrospinal fluid rather than by its becoming a substrate for a saturable efflux system. Thus, lack of transport through the BBB into the CNS, rather than efflux from the CNS, is the dominant mechanism for PEG-MLA's ability to block the uptake of endogenous leptin.

Nevertheless, the long half-life of PEG-MLA in the blood and its extreme resistance to degradation in both blood and brain suggest that even a slow rate of passage across the BBB, detected by use of radiolabeled PEG-MLA, might eventually result in therapeutic CNS levels, similar to molecules such as erythropoietin and antibodies (34, 35). Indeed, we found an extremely low rate of PEG-MLA entry into the frontal cortex, cerebellum, and hypothalamus, the latter featuring the most prominent uptake, which was higher than accounted for by leakage through the extracellular pathways. This regional pattern is similar to that found for endogenous leptin and suggests that PEG-MLA may be using and thus blocking the leptin transporter (21, 36, 37). Capillary depletion and measurement by RIA confirmed these results and demonstrated 75-fold higher PEG-MLA levels than that of endogenous brain leptin, probably high enough to compete with endogenous leptin for the arcuate nucleus receptor. Thus, PEG-MLA likely inhibits leptin activity via two mechanisms: first, by blocking the transport of circulating leptin across the BBB, thus inducing peripheral resistance and central leptin deficiency, and then by blocking the binding of any CNS leptin to its receptor, thus inducing central resistance.

The mechanism of action proposed here for PEG-MLA is consistent with theories on leptin resistance in human obesity resulting from defects in downstream neural circuitries, resistance at the arcuate nucleus receptor, or defects in BBB transport. Classic work has shown that the BBB deficit is demonstrable first (38, 39). Theoretical calculations and experimental evidence indicate that the two likely develop in tandem, with defects in BBB transport more severe than receptor resistance at most levels of

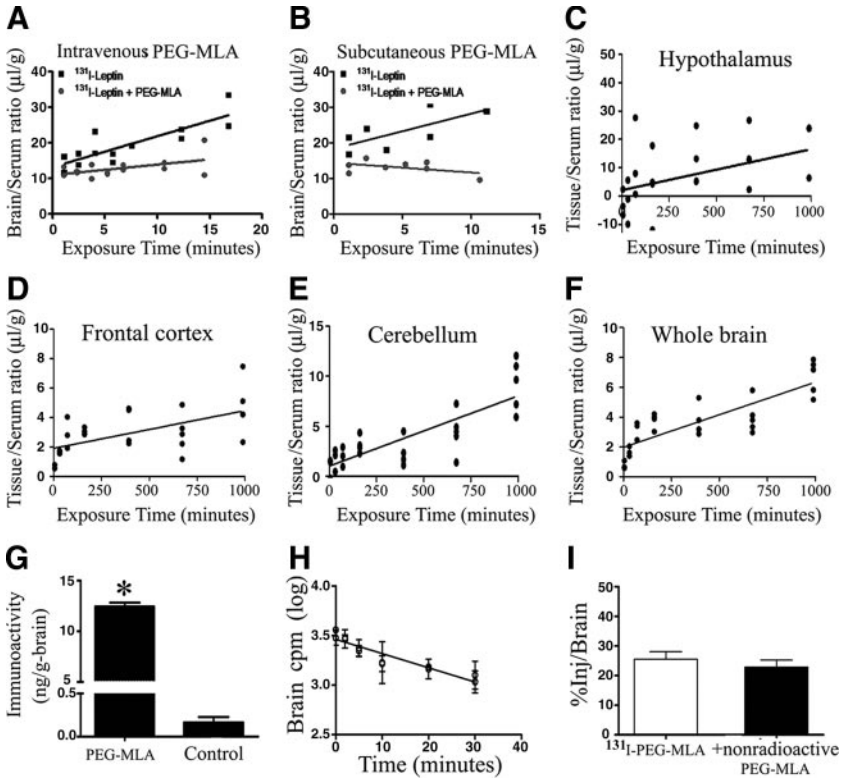

FIG. 6. Effect of PEG-MLA on blood-brain leptin transport. PEG-MLA was given iv (A) or sc (B) to test its effect on the transport of iv-administered radioactive murine leptin across the BBB. PEG-MLA administration via both routes significantly inhibited leptin transport across the BBB. C–F, Uptake of iv-administered ^{131}I-PEG-MLA into four representative brain regions over a 16-h time course. Brain-to-serum ratios were corrected for 125I-albumin ratios to compensate for leakage through extracellular pathways. Uptake was low but measurable, reaching a highest rate of $Ki = 0.0144$ in the hypothalamus. G, Brain PEG-MLA and leptin levels. Mean PEG-MLA levels in treated mice was 12.4 ± 0.42 ng/g brain, as compared to 0.17 ± 0.06 ng/g brain endogenous leptin in vehicle-treated mice ($P < 0.05$). H and I, Brain-to-blood ^{131}I-PEG-MLA efflux. Slow rate of clearance from brain (H) and lack of inhibition of unlabeled PEG-MLA on ^{131}I-PEG-MLA efflux in excess of nonlabeled PEG-MLA (I), indicate that PEG-MLA is not effluxed from the brain by a saturable system.

obesity (40, 41), suggesting that resistance at the BBB and the CNS receptor would become self-reinforcing and enter into a positive feedback loop. This is consistent with experimental work that shows that obesity arising because of receptor deficits or defects in downstream neuronal circuitries eventually leads to defects in BBB transporters (42, 43).

The severity of the BBB defect correlates with body weight and body mass index in mice with obesity of maturity, diet-induced obesity and is reversible with weight loss (44, 45). The cause of the defect is multifactorial. The saturable nature of the leptin transporter with a Michaelis constant (K_m) at about 10 ng/ml results in obese individuals having more leptin in the brain or cerebrospinal fluid than thin individuals (37, 46–48). Factors other than self-inhibition are involved in impaired leptin transport in obese individuals, suggesting that leptin transporter is not static but influenced by pathophysiological events. Leptin transport is indeed regulated by α-adrenergics, insulin, and glucose, which stimulate leptin transport, and triglycerides, which inhibit it (43, 49, 50). The lower level of leptin in the CNS would attenuate anorexia and redirect energy expenditures away from costly caloric upkeep of the immune, reproductive, and other systems (51–53).

Thus, much indirect work has implicated defects in leptin transport in obesity and has even indicated how decreased leptin transport can convey survival advantage during starvation. Whereas it was shown that primary defects in receptor function or down stream neural circuitries leads to obesity (42, 54, 55), no similar data exist for a primary BBB transport defect. Because PEG-MLA acts primarily by blocking leptin transport across BBB, our results reinforce the importance of such transport in weight control.

In conclusion, we demonstrate the effectiveness of a leptin antagonist with extended half-life for induction of a reversible state of leptin deficiency in mice, resulting in increased food intake and associated weight gain. Application of this approach may enable further study of leptin's effects on various physiological and pathological processes governed or influenced by leptin signaling. In addition, it may represent a new therapeutic modality for weight gain in states of cachexia, such as cancer, anorexia nervosa, anorexia of aging, and AIDS, in which weight loss is linked to enhanced mortality and weight gain may be associated with a survival advantage. Furthermore, PEG-MLA treatment may be used to modulate conditions that are suggested to be linked to excess leptin, such as autoimmune disorders, atherosclerosis, and liver fibrosis.

Acknowledgments

Address all correspondence and requests for reprints to: Professor Arieh Gertler, Institute of Biochemistry, Food Science, and Nutrition, The Robert H. Smith Faculty of Agriculture, Food, and the Environment, The Hebrew University of Jerusalem, P.O. Box 12, Rehovot 76100, Israel. E-mail: gertler@agri.huji.ac.il.

This work was supported by Israel Science Foundation Grants 798/05 (to E.E.) and 521/07 (to A.G. and E.E.), Veterans Affairs Merit Review and National Institutes of Health Grants R01 NS051334, R01 AG029839, and R01 050547 (to W.A.B.), and partially supported by the Weizmann Institute of Science-Tel Aviv Medical Center Research Fund (to E.E.).

Disclosure Summary: The authors have nothing to disclose.

References

1. **Zhang Y, Proenca R, Maffei M, Barone M, Leopold L, Friedman JM** 1994 Positional cloning of the mouse obese gene and its human homologue. Nature 372:425–432
2. **Karmazyn M, Purdham DM, Rajapurohitam V, Zeidan A** 2007 Leptin as a cardiac hypertrophic factor: a potential target for therapeutics. Trends Cardiovasc Med 17:206–211
3. **Peelman F, Waelput W, Iserentant H, Lavens D, Eyckerman S, Zabeau L, Tavernier J** 2004 Leptin: linking adipocyte metabolism with cardiovascular and autoimmune diseases. Prog Lipid Res 43:283–301
4. **La Cava A, Matarese G** 2004 The weight of leptin in immunity. Nat Rev Immunol 4:371–379
5. **Matarese G, Moschos S, Mantzoros CS** 2005 Leptin in immunology. J Immunol 174:3137–3142

6. **Ikejima K, Takei Y, Honda H, Hirose M, Yoshikawa M, Zhang YJ, Lang T, Fukuda T, Yamashina S, Kitamura T, Sato N** 2002 Leptin receptor-mediated signaling regulates hepatic fibrogenesis and remodeling of extracellular matrix in the rat. Gastroenterology 122:1399–1410
7. **Ramos EJ, Suzuki S, Marks D, Inui A, Asakawa A, Meguid MM** 2004 Cancer anorexia-cachexia syndrome: cytokines and neuropeptides. Curr Opin Clin Nutr Metab Care 7:427–434
8. **Mak RH, Cheung W, Cone RD, Marks DL** 2006 Mechanisms of disease: cytokine and adipokine signaling in uremic cachexia. Nat Clin Pract Nephrol 2:527–534
9. **Torsello A, Brambilla F, Tamiazzo L, Bulgarelli I, Rapetti D, Bresciani E, Locatelli V** 2007 Central dysregulations in the control of energy homeostasis and endocrine alterations in anorexia and bulimia nervosa. J Endocrinol Invest 30:962–976
10. **Elinav E, Ali M, Bruck R, Brazowsky E, Phillips A, Shapira Y, Katz M, Solomon G, Halpern Z, Gertler A** 2009 Competitive inhibition of leptin signaling results in amelioration of liver fibrosis through modulation of stellate cell function. Hepatology 49:278–286
11. **Maack T, Johnson V, Kau ST, Figueiredo J, Sigulem D** 1979 Renal filtration, transport, and metabolism of low-molecular-weight proteins: a review. Kidney Int 16:251–270
12. **Haffner D, Schaefer F, Girard J, Ritz E, Mehls O** 1994 Metabolic clearance of recombinant human growth hormone in health and chronic renal failure. J Clin Invest 93:1163–1171
13. **Fuertges F, Abuchowski A** 1990 The clinical efficacy of poly(ethylene glycol)-modified proteins. J Controlled Release 11:139–148
14. **Bailon P, Berthold W** 1998 Polyethylene glycol-conjugated pharmaceutical proteins. Pharm Sci Technol Today 1:352–356
15. **Clark R, Olson K, Fuh G, Marian M, Mortensen D, Teshima G, Chang S, Chu H, Mukku V, Canova-Davis E, Somers T, Cronin M, Winkler M, Wells JA** 1996 Long-acting growth hormones produced by conjugation with polyethylene glycol. J Biol Chem 271:21969–21977
16. **Raver N, Gussakovsky EE, Keisler DH, Krishna R, Mistry J, Gertler A** 2000 Preparation of recombinant bovine, porcine, and porcine W4R/R5K leptins and comparison of their activity and immunoreactivity with ovine, chicken, and human leptins. Protein Expr Purif 19:30–40
17. **Niv-Spector L, Gonen-Berger D, Gourdou I, Biener E, Gussakovsky EE, Benomar Y, Ramanujan KV, Taouis M, Herman B, Callebaut I, Djiane J, Gertler A** 2005 Identification of the hydrophobic strand in the A-B loop of leptin as major binding site III: implications for large-scale preparation of potent recombinant human and ovine leptin antagonists. Biochem J 391:221–230
18. **Mystkowski P, Shankland E, Schreyer SA, LeBoeuf RC, Schwartz RS, Cummings DE, Kushmerick M, Schwartz MW** 2000 Validation of whole-body magnetic resonance spectroscopy as a tool to assess murine body composition. Int J Obes Relat Metab Disord 24:719–724
19. **Patlak CS, Blasberg RG, Fenstermacher JD** 1983 Graphical evaluation of blood-to-brain transfer constants from multiple-time uptake data. J Cereb Blood Flow Metab 3:1–7
20. **Blasberg RG, Patlak CS, Fenstermacher JD** 1983 Selection of experimental conditions for the accurate determination of blood-brain transfer constants from single-time experiments: a theoretical analysis. J Cereb Blood Flow Metab 3:215–225
21. **Banks WA, Kastin AJ, Huang W, Jaspan JB, Maness LM** 1996 Leptin enters the brain by a saturable system independent of insulin. Peptides 17:305–311
22. **Triguero D, Buciak J, Pardridge WM** 1990 Capillary depletion method for quantification of blood-brain barrier transport of circulating peptides and plasma proteins. J Neurochem 54:1882–1888
23. **Gutierrez EG, Banks WA, Kastin AJ** 1993 Murine tumor necrosis factor α is transported from blood to brain in the mouse. J Neuroimmunol 47:169–176
24. **Banks WA, Kastin AJ, Fischman AJ, Coy DH, Strauss SL** 1986 Carrier-mediated transport of enkephalins and N-Tyr-MIF-1 across blood-brain barrier. Am J Physiol 251:E477–E482
25. **Elinav E, Waks T, Eshhar Z** 2008 Redirection of regulatory T cells with predetermined specificity for the treatment of experimental colitis in mice. Gastroenterology 134:2014–2024
26. **Wang YS, Youngster S, Grace M, Bausch J, Bordens R, Wyss DF** 2002 Structural and biological characterization of pegylated recombinant interferon α-2b and its therapeutic implications. Adv Drug Deliv Rev 54:547–570
27. **Bailon P, Palleroni A, Schaffer CA, Spence CL, Fung WJ, Porter JE, Ehrlich GK, Pan W, Xu ZX, Modi MW, Farid A, Berthold W, Graves M** 2001 Rational design of a potent, long-lasting form of interferon: a 40 kDa branched polyethylene glycol-conjugated interferon α-2a for the treatment of hepatitis C. Bioconjug Chem 12:195–202
28. **Myers MG, Cowley MA, Munzberg H** 2008 Mechanisms of leptin action and leptin resistance. Annu Rev Physiol 70:537–556
29. **Cnop M, Landchild MJ, Vidal J, Havel PJ, Knowles NG, Carr DR, Wang F, Hull RL, Boyko EJ, Retzlaff BM, Walden CE, Knopp RH, Kahn SE** 2002 The concurrent accumulation of intra-abdominal and subcutaneous fat explains the association between insulin resistance and plasma leptin concentrations: distinct metabolic effects of two fat compartments. Diabetes 51:1005–1015
30. **Johannsson G, Karlsson C, Lonn L, Marin P, Bjorntorp P, Sjostrom L, Carlsson B, Carlsson LM, Bengtsson BA** 1998 Serum leptin concentration and insulin sensitivity in men with abdominal obesity. Obes Res 6:416–421
31. **Sudi KM, Gallistl S, Tafeit E, Moller R, Borkenstein MH** 2000 The relationship between different subcutaneous adipose tissue layers, fat mass and leptin in obese children and adolescents. J Pediatr Endocrinol Metab 13:505–512
32. **Tai ES, Lau TN, Ho SC, Fok AC, Tan CE** 2000 Body fat distribution and cardiovascular risk in normal weight women. Associations with insulin resistance, lipids and plasma leptin. Int J Obes Relat Metab Disord 24:751–757
33. **Misra A, Vikram NK** 2003 Clinical and pathophysiological consequences of abdominal adiposity and abdominal adipose tissue depots. Nutrition 19:457–466
34. **Banks WA** 2004 Are the extracellular [correction of extracellular] pathways a conduit for the delivery of therapeutics to the brain? Curr Pharm Des 10: 1365–1370
35. **Banks WA** 2006 The CNS as a target for peptides and peptide-based drugs. Expert Opin Drug Deliv 3:707–712
36. **Banks WA** 2004 The many lives of leptin. Peptides 25:331–338
37. **Banks WA, Clever CM, Farrell CL** 2000 Partial saturation and regional variation in the blood-to-brain transport of leptin in normal weight mice. Am J Physiol Endocrinol Metab 278:E1158–E1165
38. **Halaas JL, Boozer C, Blair-West J, Fidahusein N, Denton DA, Friedman JM** 1997 Physiological response to long-term peripheral and central leptin infusion in lean and obese mice. Proc Natl Acad Sci USA 94:8878–8883
39. **Van Heek M, Compton DS, France CF, Tedesco RP, Fawzi AB, Graziano MP, Sybertz EJ, Strader CD, Davis Jr HR** 1997 Diet-induced obese mice develop peripheral, but not central, resistance to leptin. J Clin Invest 99:385–390
40. **El-Haschimi K, Pierroz DD, Hileman SM, Bjorbaek C, Flier JS** 2000 Two defects contribute to hypothalamic leptin resistance in mice with diet-induced obesity. J Clin Invest 105:1827–1832
41. **Banks WA, Lebel CR** 2002 Strategies for the delivery of leptin to the CNS. J Drug Target 10:297–308
42. **Levin BE, Dunn-Meynell AA, Banks WA** 2004 Obesity-prone rats have normal blood-brain barrier transport but defective central leptin signaling before obesity onset. Am J Physiol Regul Integr Comp Physiol 286:R143–R150
43. **Banks WA** 2001 Enhanced leptin transport across the blood-brain barrier by α1-adrenergic agents. Brain Res 899:209–217
44. **Banks WA, Kastin AJ, Brennan JM, Vallance KL** 1999 Adsorptive endocytosis of HIV-1gp120 by blood-brain barrier is enhanced by lipopolysaccharide. Exp Neurol 156:165–171
45. **Banks WA, Farrell CL** 2003 Impaired transport of leptin across the blood-brain barrier in obesity is acquired and reversible. Am J Physiol Endocrinol Metab 285:E10–E15
46. **Caro JF, Kolaczynski JW, Nyce MR, Ohannesian JP, Opentanova I, Goldman WH, Lynn RB, Zhang PL, Sinha MK, Considine RV** 1996 Decreased cerebrospinal-fluid/serum leptin ratio in obesity: a possible mechanism for leptin resistance. Lancet 348:159–161
47. **Schwartz MW, Peskind E, Raskind M, Boyko EJ, Porte Jr D** 1996 Cerebrospinal fluid leptin levels: relationship to plasma levels and to adiposity in humans. Nat Med 2:589–593
48. **Mantzoros C, Flier JS, Lesem MD, Brewerton TD, Jimerson DC** 1997 Cerebrospinal fluid leptin in anorexia nervosa: correlation with nutritional status and potential role in resistance to weight gain. J Clin Endocrinol Metab 82:1845–1851
49. **Banks WA, Coon AB, Robinson SM, Moinuddin A, Shultz JM, Nakaoke R, Morley JE** 2004 Triglycerides induce leptin resistance at the blood-brain barrier. Diabetes 53:1253–1260
50. **Kastin AJ, Akerstrom V** 2001 Glucose and insulin increase the transport of leptin through the blood-brain barrier in normal mice but not in streptozotocin-diabetic mice. Neuroendocrinology 73:237–242
51. **Ahima RS, Prabakaran D, Mantzoros C, Qu D, Lowell B, Maratos-Flier E, Flier JS** 1996 Role of leptin in the neuroendocrine response to fasting. Nature 382:250–252
52. **Cheung CC, Thornton JE, Kuijper JL, Weigle DS, Clifton DK, Steiner RA** 1997 Leptin is a metabolic gate for the onset of puberty in the female rat. Endocrinology 138:855–858
53. **Lord GM, Matarese G, Howard JK, Baker RJ, Bloom SR, Lechler RI** 1998 Leptin modulates the T cell immune response and reverses starvation-induced immunosuppression. Nature 394:897–901
54. **Cohen P, Zhao C, Cai X, Montez JM, Rohani SC, Feinstein P, Mombaerts P, Friedman JM** 2001 Selective deletion of leptin receptor in neurons leads to obesity. J Clin Invest 108:1113–1121
55. **Schwartz MW, Woods SC, Porte Jr D, Seeley RJ, Baskin DG** 2000 Central nervous system control of food intake. Nature 404:661–671